HHS Public Access

Author manuscript

Exp Cell Res. Author manuscript; available in PMC 2022 March 01.

Published in final edited form as:

Exp Cell Res. 2021 March 01; 400(1): 112508. doi:10.1016/j.yexcr.2021.112508.

Noonan syndrome patient-specific induced cardiomyocyte model carrying SOS1 gene variant c.1654A>G

Narasimman Gurusamy[1], **Sheeja Rajasingh**[1], **Vinoth Sigamani**[1], **Reshma Rajasingh**[2], **Dona Greta Isai**[3], **Andras Czirok**[3], **Douglas Bittel**[4], **Johnson Rajasingh**[1,5,6,*]

[1]Department of Bioscience Research, University of Tennessee Health Science Center, Memphis, TN

[2]Dartmouth College, Hanover, NH,

[3]Department of Anatomy and Cell Biology, University of Kansas Medical Center, Kansas City, KS

[4]Children's Mercy Hospital, Kansas City, MO

[5]Department of Medicine-Cardiology, University of Tennessee Health Science Center, Memphis, TN

[6]Department of Microbiology, Immunology & Biochemistry, University of Tennessee Health Science Center, Memphis, TN

Abstract

Noonan syndrome (NS) is a dominant autosomal genetic disorder, associated with mutations in several genes that exhibit multisystem abnormal development including cardiac defects. NS associated with the Son of Sevenless homolog 1 (SOS1) gene mutation attributes to the development of cardiomyopathy and congenital heart defects. Since the treatment option for NS is very limited, an in vitro disease model with SOS1 gene mutation would be beneficial for exploring therapeutic possibilities for NS. We reprogrammed cardiac fibroblasts obtained from a NS patient and normal control skin fibroblasts (C-SF) into induced pluripotent stem cells (iPSCs). We identified NS-iPSCs carry a heterozygous single nucleotide variation in the SOS1 gene at the c.1654A>G. Furthermore, the control and NS-iPSCs were differentiated into induced cardiomyocytes (iCMCs), and the electron microscopic analysis showed that the sarcomeres of the NS-iCMCs were highly disorganized. FACS analysis showed that 47.5 % of the NS-iCMCs co-expressed GATA4 and cardiac troponin T proteins, and the mRNA expression levels of many cardiac related genes, studied by qRT-PCR array, were significantly reduced when compared

[*]Address correspondence to: **Johnson Rajasingh, PhD**, Associate Professor, Department of Bioscience Research, Department of Medicine-Cardiology, Department of Microbiology, Immunology and Biochemistry, University of Tennessee Health Science Center, 847 Monroe Avenue, Memphis, TN 38163, rjohn186@uthsc.edu, Phone: 901-448-3358.

Author Contributions: "Conceptualization, J.R.; methodology, N.G, S.R., V.S., R.R., D.G.I., A.C.; software, D.G.I., A.C., D.B., S.R.; validation and formal analysis, S.R. writing-original draft preparation, N.G., V.S., S.R. A.C.; writing-review and editing, J.R., R.R., S.R.; supervision, J.R..; project administration, S.R.; funding acquisition, J.R. All authors have read and agreed to the current version of the manuscript."

Conflicts of Interest: The authors declare no conflict of interest.

to the control C-iCMCs. We report for the first time that NS-iPSCs carry a single nucleotide variation in the SOS1 gene at the c.1654A>G were showing significantly reduced cardiac genes and proteins expression as well as structurally and functionally compromised when compared to C-iCMCs. These iPSCs and iCMCs can be used as a modeling platform to unravel the pathologic mechanisms and also the development of novel drug for the cardiomyopathy in patients with NS.

Keywords

Noonan syndrome; SOS1 gene; induced pluripotent stem cells; induced cardiomyocytes; cardiomyopathy

Introduction

Noonan syndrome (NS) is an autosomal dominant genetic disorder that prevents normal development and brings about unusual body and facial characteristics, short stature, and congenital heart defects, including pulmonic valve stenosis, hypertrophic cardiomyopathy, and atrioventricular septal defects (1). The occurrence of this disorder is estimated to be in 1/1000–2500 live births (2). Congenital heart defects and their associated cardiomyopathy in NS are known to cause significant morbidity and mortality (3). Mutations in several genes have been identified in association with NS. Typically, the genes involved in causing disturbances in the RAS-MAP kinase signaling pathways are known to elicit the symptoms of NS (3). Germline mutations found in the genes of protein-tyrosine phosphatase, nonreceptor-type 11 (*PTPN11*), kirsten rat sarcoma viral oncogene homolog (*KRAS*), Son of Sevenless homolog 1 (*SOS1*), v-raf-1 murine leukemia viral oncogene homolog 1 (*RAF1*), SHOC2 leucine rich repeat scaffold protein (*SHOC2*), neuroblastoma RAS viral oncogene homolog (*NRAS*), Casitas B-lineage Lymphoma (*CBL*), *V*-Raf murine sarcoma viral oncogene homolog B1 (*BRAF*) and mitogen activated protein kinase 1 (*MAP2K1*) are responsible for the cause of approximately 75%–80% NS patients (4). The *SOS1* gene mutation is considered one of the main molecular causes, and about 20% of NS patients carry this mutation (5). Patients with the *SOS1* mutations also display a unique phenotype with frequent ectodermal anomalies (5). Functionally, SOS1 is a multi-domain protein as well as a RAS-specific guanine nucleotide exchanger factor that assists in the transformation of RAS from its inactive GDP- bound form to its active GTP-bound form (6). Currently, the treatment option for NS associated cardiomyopathy is very limited, and the availability of autologous cardiomyocytes (CMCs) from the diseased patients is scarce. Successful generation of induced pluripotent stem cells (iPSCs), differentiation towards CMCs from a NS patient's fibroblast, high-throughput molecular screening of cells, and drug testing provide hope for the treatment and identification of this disease's biological mechanisms. These advances have been instrumental in helping us understand rare disorders and reassure patients and their parents through the identification of the biologic basis for these diseases. Thus, the focus needs to be on the development of a model that replicates the phenotype at the cellular level. The generation of induced pluripotent stem cells (iPSCs) from the NS patient-specific cells holds promise for an increased understanding of this genetic disease and may also expedite the development of novel therapeutic interventions and therapeutic targets. In this study, we have generated a human iPSC line using cardiac

fibroblast cells from a patient with NS. For reprogramming, we employed non-integrating, xeno-free and non-viral transfection techniques that used a critical combination of mRNAs of pluripotency transcription factors. Furthermore, we characterized that the NS patient-derived cells including the iPSCs carry a single nucleotide variation in the SOS1 gene at the c.1654A>G. This iPSC line offers a valuable platform for a cell-based model for the drug development to treat NS. Since NS is often associated with cardiomyopathy, we have further differentiated the iPSCs into induced cardiomyocytes (iCMCs) using our previously established protocol (7). These iCMCs derived from NS patient were defective in their sarcomere organization and contractile function. These NS-iCMCs can be used as a model to study the disease mechanisms and identify a novel drug for NS associated cardiomyopathy.

Materials and Methods

Antibodies and reagents

We used primary antibodies for Oct4, Nanog, Sox2, tropomyosin 1 (Cell Signaling Technology), β-actin, Tra1–60, Tra1–81, SSEA4, cardiac troponin T, and alpha sarcomeric actin (Santa Cruz Biotechnology, Inc.) to perform in vitro analysis. Secondary antibodies such as HRP-conjugated donkey anti–mouse, anti–rabbit, anti–goat (Santa Cruz Biotechnology, Inc.); TRITC-, FITC-, and Cy-5-conjugated donkey anti–mouse, anti–goat, and anti–rabbit (Jackson Immunoresearch Laboratories, Inc.) were used. DAPI (Life-Tech); Matrigel (BD Biosciences) NutriStem medium, alkaline phosphatase assay kit (Stemgent, Cambridge, MA); RPMI medium, Mytomycin C (Sigma-Aldrich, USA). StemRNA Reprogramming kit (Reprocell USA Inc).

Cell culture

Normal human skin fibroblasts (SF) that served as control were obtained from ATCC (ATCC CRL-4001, derived from a neonatal male) and the NS patient-specific cardiac fibroblast cells were obtained from a female baby who had a heterozygous single-gene defective mutation in the SOS1 gene (NS-CF), provided by Dr. Douglas Bittel, Children's Mercy Hospital, Kansas City, KS. The DNA sequencing analysis showed that the single-gene mutation is at the level of p.Arg522Gly (c.1654 A>G). These cells were cultured in a DMEM medium at 37°C with humidified air in a 5% CO2 incubator. The iPSCs were cultured on Matrigel-coated plates in NutriStem medium at 37°C with humidified air in a 5% CO2 incubator. The iCMCs were cultured with RPMI medium, supplemented with ascorbic acid and human serum albumin (0.05%) at 37°C with humidified air in a 5% CO2 incubator. All the cells were passaged using Typsin LE (Sigma, USA).

Non-viral reprogramming of fibroblasts into iPSCs

For the generation of iPSCs, we have cultured normal control SFs (C-SFs) and NS-cardiac fibroblasts (NS-CFs) at a density of 5000 cells per well in a 6-well dish coated with iMatrix in NutriStem medium. These cells were reprogrammed into iPSCs, as described in our earlier publications, with some modifications [7]. Briefly, the cells were transfected daily with the mRNA of Oct4, Sox2, Klf4, cMyc, Nanog and Lin28 with the help of transfecting agent, lipofectamine along with a cocktail of microRNAs (Reprocell USA Inc) for 10 days. From day 13, in both control SFs and NS-CFs, we have observed that several

iPSC granulated colonies in the culture dish. The generated iPSC positive colonies were identified by live staining with Tra1–60. These Tra1–60 positive colonies were manually picked and subcultured in a Matrigel-coated plate for ten passages before being used for further analysis.

Differentiation of iPSCs into CMC

To induce the differentiation of iPSCs into iCMCs, we followed the same protocol as described earlier with minor modifications (7). Briefly, the iPSCs were cultured in NutriStem medium in a Matrigel-coated 6-well plate (BD biosciences) for a few days. When the cells reached 80–90% confluence, these cells were treated with iPSC medium containing 5μM GSK inhibitor CHIR99021 (Tocris Bioscience) and bFGF (10 ng/ml) for two days, followed by RPMI medium containing ascorbic acid (213 μg/ml) and Wnt inhibitor (2 μM of WntC59, Tocris Bioscience) supplemented with 0.05% human serum albumin for five subsequent days. We observed the beating of the iCMCs in culture from day six onwards.

Differentiation of iPSCs into Endoderm cells

In order to differentiate the iPSCs into endoderm, we adapted differentiating monolayer cultures using the STEMdiff definitive endoderm kit (Catalog #05110) from Stemcell Technologies and followed the procedures as per the manufacturer's instructions. The cells were collected on day-14 and washed with PBS. RNA was then isolated using Trizol, and the expression of endoderm specific markers were studied using qPCR.

Differentiation of iPSCs into Neuronal cells

In order to differentiate the iPSCs into neuronal cells, we utilized the STEMdiff SMADi neural induction kit (Catalog #08581) from Stemcell Technologies and followed the procedures as per the manufacturer's instructions. The cells were collected on day-18, after being washed with PBS. RNA was isolated using Trizol, and the expression of neuronal markers were studied using qPCR.

Western blot analysis

The Western blot analyses for the expression of Oct4, Sox2, and Nanog proteins were performed to see the iPSCs. Another analysis was performed for the expression of cardiac troponin T, cardiac troponin I, and tropomyosin 1 proteins using iCMCs as described by us earlier (7). The antibodies were purchased from Cell Signaling Technology, USA.

Quantitative RT-PCR

We performed the qRT-PCR analysis for stem cell pluripotent genes in iPSCs, and for the cardiac specific genes in iCMCs. The iPSCs and the iCMCs from a six-well plate were washed once with phosphate-buffered saline (PBS) and harvested for qRT-PCR analysis as described earlier (7). The total cellular RNA was isolated using Trizol reagent and converted into cDNA using High-Capacity cDNA Reverse Transcription Kit (Applied Biosystems). PowerUp SYBR Green Master Mix and TaqMan Master Mix were employed for the amplification and detection of qPCR products using QuantStudio 6 Pro real time PCR (Applied Biosystems). The gene expression profiles of the primer sequences are given

in Table 1 and 2. The relative mRNA expression of target genes was normalized to the endogenous 18S control gene (Applied Biosystems). The results were expressed as fold change and the values were calculated as the ratio of induced expression-to-control expression. For the comparative expression of cardiac genes in iCMCs, we have utilized GeneQuery Human Cardiac Myocyte Biology qPCR array kit from ScienCell Research Laboratories (catalogue number GK098).

Immunofluorescence staining

We performed immunofluorescence analysis for stem cell pluripotent genes in iPSCs, and cardiac specific genes in iCMCs grown in 8-well chamber slides that were washed three times with phosphate-buffered saline (PBS) as described by us earlier (7). iPSCs and iCMCs were fixed in 4% paraformaldehyde for 5 min, rinsed with Dulbecco's phosphate-buffered saline (DPBS), and permeabilized with 0.1% TritonX-100 in DPBS for 3 minutes. The cells were then blocked with blocking buffer for 30 minutes, and then incubated with primary antibodies overnight at 4°C. After three times washing with DPBS, a corresponding secondary antibody was added to the cells and incubated for 1 hour at 37°C incubator. After washing with DPBS for three times, the cells were stained with DAPI and used for analysis. All immunofluorescence staining was photographed using either a confocal or immunofluorescence microscope.

Particle Image Velocimetry (PIV) Analysis

The functional characteristics of differentiated iCMCs were measured using PIV analysis that assessed the spatiotemporal pattern of cardiomyocyte contractile activity, as described by us earlier (7, 8). We examined the cell contractility using an image cross-correlation algorithm analysis. High frame rate (10 frames/sec) movies were recorded in a temperature-controlled atmosphere. We used 20x objectives, both in phase contrast and bright field modes. A movement pattern (velocity field) captured on a pair of images was analyzed using the method described earlier (7, 8).

Flow cytometry analysis

Flow cytometry analysis was performed to characterize the iPSC phenotypes using primary antibodies anti-Oct4, and anti-Sox2, and iCMCs using anti-TNNT2 and anti-Gata4 as described earlier (7). Cells from a six-well plate were harvested and washed twice in PBS. The cells were then counted and fixed with 4% paraformaldehyde for 3 minutes at room temperature before being washed with DPBS and permeabilized with 0.1% TritonX-100 in DPBS for 3 minutes. The cells were then blocked with blocking buffer for 30 minutes. Subsequently, the cells were incubated with the appropriately labeled primary antibodies for 1 hour. Next, the cells were washed with washing buffer three times followed by incubation for 20 minutes with an appropriate secondary antibody. All incubations were performed on ice. Appropriate isotype controls were used for all cases. Finally, the cells were washed three times with FACS buffer, resuspended in 0.5 ml PBS, and the cells were analyzed by a flow cytometer (FACSCalibur, BD Biosciences). Data were analyzed by using FlowJo software (Tree Star, Ashland, OR).

Confirmation of single nucleotide variant by PCR-RFLP and Sanger Sequencing

Polymerase chain reaction-restriction fragment length polymorphism (PCR-RFLP) and Sanger sequencing were performed to confirm the single nucleotide variant in the SOS1 gene at c.1654A>G in the NS-iPSCs. First, the DNA was isolated from the C-iPSCs, NS-iPSCs and from the cardiac fibroblasts of the NS patient by using the DNeasy Blood & Tissue Kit (Qiagen). PCR was performed by using gene-specific primers (SOS1_F – 5`-ACACGTGTAGGAGCCAAACA-3` and SOS_R – 5`-TGGCTTCCAGGATTGCAACA-3`) designed with Primer3 software to spin around the 996bp of the SOS1 gene variant (rs137852814). The PCR product was purified with a QIAquick PCR purification kit (Qiagen) and resolved in 1% agarose gel electrophoresis. Then 20μl of the PCR product was digested with 2U of restriction enzyme (*Hpy*AV), 5μl of 10X NEBuffer, and made-up the volume to 50 μl with sterile distilled water. Then the reaction mixture was incubated at 37° C for 15 minutes in a thermal cycler, and the product was resolved in 2% agarose gel electrophoresis. Sanger sequencing was performed using the above PCR product with SOS1_F primer in order to confirm the presence of SOS1 gene variant through GeneArt support (Thermofisher).

Telomere length quantification

Absolute telomere length in the NS-patient derived iPSCs and their parent cells was analyzed using the human telomere length quantification qRT-PCR assay kit from ScienCell Research Laboratories as per the directions provided in the manufacturer protocol (Cat. No: 8918). This kit is designed to measure the absolute telomere length of a human cell population.

Institutional regulatory approval

Cryopreserved de-identified NS patient-specific cardiac fibroblast cells were obtained from Dr. Douglas Bittel, Children's Mercy Hospital, Kansas City, MO. All methods pertaining to human samples were carried out in accordance with relevant guidelines, and regulations were approved by the institutional review board of Children's Mercy Hospital and my previous work institution, the University Kansan Medical Center, Kansas City, KS.

Statistical analysis

All experiments were repeated at least 3 times. Results are presented as mean±SEM. Comparisons were performed by one-way ANOVA (Graphpad Prism) and probability values less than 0.05 were considered statistically significant.

Results

Generation of iPSCs from Noonan syndrome patient:

We observed that sequential cell morphological changes occurred during the reprogramming of NS-CFs into NS-iPSCs. Our phase-contrast microscopic images showed a significant cell transition during the reprogramming of NS-CFs into iPSCs from days 0, 5, 7, and 11 (Supplemental Fig. S1 A-D). On day-13, there were true iPSC colonies generated from the NS-CFs which were similar to the pluripotent stem cell colonies (Supplemental Fig.

S1 E). To identify the real iPSC colonies, we used the Tra1–60 live fluorescence staining antibody (Stemgent). The immunofluorescence image showed that the endogenous Tra1–60 gene was expressed in NS-iPSCs (Supplemental Fig. S1 F). Moreover, these colonies were positive for alkaline phosphatase staining (Supplemental Fig. S1 G). We have selected three independent iPSC clones for both control and NS-patient derived cells for further analysis. In addition, the transmission electron microscopic images delineated the nuclear morphology of iPSCs, where the nuclear membrane was smooth and rounded in SF-iPSCs, and it was rumpled in NS-iPSCs (Supplemental Fig. S1 H-I). These data clearly show that there was no morphological difference between control and NS derived iPSCs, whereas, we have observed significant ultrastructural changes in the nucleus of NS-iPSCs.

Characterization of the pluripotency of iPSCs derived from NS patient

We further characterized all the three iPSC clones obtained from control and NS-patient derived cells by examining their expression of pluripotency genes. Our comparative quantitative real-time PCR analysis showed that the mRNA expressions of the pluripotency genes OCT4, Nanog and Sox2 were significantly higher in both control C-iPSCs and NS-iPSCs when compared to their respective parent cells (Fig. 1A). Besides that, there were no significant differences in the expressions of pluripotency genes between the iPSCs derived from control and NS patients (Fig. 1A). To see the protein expression of pluripotent genes in NS-iPSCs, we performed Western blot and flow cytometry analyses at passage 9 (P-9). Western blot analysis showed that the protein of important pluripotent genes Oct4, Sox2 and Nanog were highly expressed in NS-iPSCs (Fig. 1B). To identify the purity of NS-iPSCs colonies, we performed flow cytometric analysis. Our flow cytometry data showed that 69 % of cells are co-expressing Oct4 and Sox2, whereas 75.5 % and 79.2% of cells are expressing SOX2 and OCT4 respectively in NS-iPSCs (Fig. 1C). The pluripotent mRNA gene expression was further supported by the protein expression by immunofluorescence image analysis. Our data showed that Nanog, Oct4, and the stage-specific embryonic antigen-4 (SSEA4) are highly expressed in NS-iPSCs (Fig. 1D-E). As we know the primary NS-CF had limited proliferation potential whereas the NS-iPSCs were very proliferatives in nature. To see the difference in telomere length between the NS-CF and NS-iPSCs, we performed an absolute telomere length quantification assay by qRT-PCR analysis. We got the telomere length of 462 ± 44 kb and 863 ± 83 kb in NS-CF and NS-iPSC, respectively in a diploid cell. Our data clearly showed that the average telomere length of target genomic DNA per diploid cell in the NS-iPSCs was significantly increased when compared to its parent NS-CFs (Fig. 1F).

Tri-lineage differentiation capabilities of NS-iPSCs

In order to demonstrate the trilineage differentiation (ectoderm, endoderm and mesoderm) capabilities of NS-iPSCs, they were cultured in the cardiac-specific medium for mesoderm differentiation, neuronal-specific medium for ectoderm differentiation and hepatocyte specific medium for endoderm differentiation for 14 days. Then the cells were analyzed for the lineage-specific genes by qRT-PCR and for proteins by immunofluorescence staining. The expression of cardiac genes GATA4 and TNNT2 (Fig. 2A) for mesodermal lineage, hepatocytes genes SOX17, AFP and APOA1 for endodermal lineage (Fig. 2B), and the neuronal marker genes MAP2 and OLIG2 (Fig. 2C) for ectodermal lineage

were significantly increased in the cells that were cultured in their differentiation medium correspondingly. The gene expression was further supported by the hepatocyte specific protein expression of alpha feto protein (AFP) (Fig. 2D) and the neuronal and astrocyte specific protein expression of nestin and GFAP, respectively (Fig. 2E). We have performed genotyping analysis which is specific for identifying the genetic mutation instead karyotyping analysis for the iPSC clones (Fig. 3). Altogether, our experiments have demonstrated a high expression of pluripotency genes, an increased telomere length, the trilineage differentiation capabilities of NS-iPSCs and satisfied all the requirements of pluripotent stem cells.

Identification of mutation at SOS1 gene mutation in NS patients

In order to confirm the SOS1 gene specific mutation in the iPSCs derived from NS patient, we have employed the polymerase chain reaction--restriction fragment length polymorphism (PCR-RFLP) and Sanger Sequencing methodologies. SOS1 gene-specific primers surrounding the SNP at the c.1654A>G (rs137852814) were designed to amplify 996 bp. The PCR product was resolved in 1% agarose gel (Fig. 3A), which showed that the C-SF, NS-CF and NS-iPSCs had amplified 996 bp of DNA. The above PCR product was further cleaved with *Hpy*AV (a type IIS restriction enzyme that recognizes asymmetric DNA sequences and cleaves outside of their recognition sequence). The resultant product was resolved in 2% agarose gel (Fig. 3B). The C-SF yielded an uncut band around 996bp (because of the presence of homozygous wild-type allele A/A), whereas the NS-iPSCs and NS-CFs have yielded three-bands of 996bp, 701bp and 294bp (because of the presence of heterozygous mutant type (A/G) (Fig. 3B). The sequencing of the SOS1 gene-specific PCR product (Fig. 3C), and multiple sequence alignments in Clustal Omega (Fig. 3D) further confirm that the C-SF had homozygous wild-type (A/A), and the NS-iPSCs and NS-CF have a heterozygous mutant-type (A/G) at coding sequence number 1654 of the SOS1 gene. Taken together, our results have confirmed that the NS-iPSCs show the presence of a heterozygous SNP variant in the SOS1 gene at the c.1654A>G even after undergoing reprogramming.

Cardiac specific genes are significantly lower in NS-iCMCs

The congenital heart defects as well as the cardiomyopathy associated with NS results in significant morbidity and mortality (9). In order to study the NS-associated cardiac effects, we induced the differentiation of iPSCs into cardiomyocytes, as described by us earlier (7). We observed the spontaneous beating of iCMCs from day six onwards. The day-14 iCMCs were harvested for cardiac-specific mRNA and protein analyses. qRT- PCR analyses have revealed that the mRNA expression of cardiac genes such as GATA4 (Fig. 4A), and cardiac troponin T (TNNT2) (Fig. 4B) were increased in both C-iCMCs and NS-iCMCs. However, the expression of GATA4, and TNNT2 were lesser in the NS-iCMCs compared with the control C-iCMCs (Fig. 4A-B). Furthermore, the mRNA expression of the hyperpolarization-activated cyclic nucleotide gated potassium channel 4 (HCN4) (Fig. 4C) and the α-sarcomeric actinin (ACTN2) (Fig. 4D) were significantly lower in NS-iCMCs when compared with the C-iCMCs. Western blotting analyses also showed that the protein expression of tropomyosin1 (TPM1), cardiac troponin T and cardiac troponin I (TNNI3) were significantly reduced in NS-iCMCs compared with the control C-iCMCs (Fig. 4E).

FACS analysis data revealed that about 47.5 % of double positive NS-iCMCs expressed GATA4 and TNNT2 (Fig. 4F). These data strongly suggest that the expression of cardiac genes and proteins were significantly reduced in NS-iCMCs.

The ultrastructural image analysis of day 14 demonstrates that the NS-iMCS were structurally disorganized

In addition, immunofluorescence microscopic image analysis revealed that the expression of alpha sarcomeric actinin (ACTN2) was lower in NS-iCMCs when compared with the control C-iCMCs (Fig. 5A-B). Furthermore, to analyze the structural maturity of iCMCs, 14-day iCMCs were examined by transmission electron microscopy (TEM), which showed that the sarcomeres were properly organized and well aligned along the myofibrils in C-iCMCs (Fig. 5C), whereas in NS-iCMCs, they were hypertrophied and contained disordered sarcomeres with irregular striations (Fig. 5D). We have observed at least 50 iCMCs per group, and noted that the iCMCs derived from control did not display any disorganized sarcomeres, whereas about 80% of the iCMCs from NS patient displayed disorganized sarcomere structures under TEM image analysis. Moreover, the nucleus appeared normal in C-iCMCs (Fig. 5E), whereas the nucleus was big and the nuclear membrane was abnormal and folded in NS-iCMCs (Fig. 5F). We have also quantified the area of the nucleus using the DAPI-stained immunofluorescence images of C-iCMCs and NS-iCMCs with ImageJ software tools. Our results showed that the average nuclear area was significantly increased in NS-iCMCs compared to C-iCMCs (supplemental Fig. S2). These microscopic images clearly indicate that NS-iCMCs were structurally disorganized.

Reduced level of cardiac genes were expressed in NS-iCMCs when compared to C-iCMCs

To gain more insight into the biology of NS-iCMCs, the mRNA expression profiles of several cardiac myocyte genes were studied using qPCR array in control NS-iCMCs and NS-iCMCs. Three samples from each group were analyzed through qPCR array, and the mean expression levels are shown as a heatmap analysis (Fig. 6A-F). The level of expression of each gene was normalized with GAPDH, and the fold-change in gene expression in iCMCs were normalized with their respective parent cell types. The average gene expression levels in the groups of C-iCMCs and NS-iCMCs, and their statistically significant values were given as Supplemental Table 1. The results of the qPCR array have been classified based on the level of expression genes. Tropomyosin1 (TPM1) expression was drastically down regulated, and atrial natriuretic factor (NPPA) and α-sarcomeric actin (ACTC1) were upregulated in NS-iCMCs (Fig. 6A). As shown in Fig. 6B, several cardiac structural genes such as cardiac α-myosin heavy chain (MYH6), β-myosin heavy chain (MYH7), desmin (DES), cardiac myosin-binding protein C (MYBPC3), cysteine and glycine-rich protein 3 (CSRP3 or cardiac LIM Protein), and the cardiac regulatory molecules like GATA4, VANGL planar cell polarity protein 2 (VANGL2), WW domain containing transcription regulator 1 (WWTR1) have been markedly decreased in NS-iCMCs. Fig. 6C shows that out of 16 cardiac genes studied, 14 genes were down regulated and 2 genes (the transcription factors HAND2 and MEF2C) were upregulated in NS-iCMCs, compared with control patient-derived iCMCs. Several ion channel-related genes such as voltage-gated calcium-channel alpha 1 subunit (CACNA1D), calcium/calmodulin dependent protein kinase II beta (CAMK2B), potassium inwardly rectifying channel subfamily J member 5 (KCNJ5), and

sodium voltage-gated channel alpha subunit 5 (SCN5A) were decreased whereas, integrin subunit alpha 1 (ITGA1), Myozenin 2 (MYOZ2) and TWIST1 were increased in NS-iCMCs (Fig. 6D). Out of 17 cardiac genes studied, 16 genes were down regulated, but the calcium voltage-gated channel subunit alpha1 S (CACNA1S) was upregulated in NS-iCMCs (Fig. 6E). As shown in Fig. 6F, out of 22 cardiac genes studied, 20 genes were markedly downregulated and 2 genes were slightly upregulated in NS-iCMCs, compared with control C-iCMCs.

Contractility assessed by particle image velocimetry (PIV) method showed NS-iCMCs were functionally compromised

To study the functional characteristics of the iCMCs derived from the normal control and NS-iPSCs, we performed a non-invasive optical assay involving the measurement of the particle image velocimetry of video microscopic recordings. The spontaneous beating of iCMCs started from day six onwards. The beating patterns of the iCMCs derived from normal control and NS patients were recorded on day-14 and are available as a supplementary video file (Video. 1 & 2). Fig. 7A and 7B show representative video microscopic fields from the C-iCMCs and NS-iCMC cultures, respectively. Representative beat patterns of C-iCMCs (Fig. 7C) and NS-iCMC cultures (Fig. 7D) indicate a regular and arrhytmic beating activity, respectively. Statistical analysis of beat patterns from n=6 recordings (Fig. 7C and D) indicates a slightly (40%) reduced beating frequency of iCMCs derived from NS patient – the difference is not statistically significant due to the large variation in the beat duration in NS-iCMCs. The 7-fold increased variability ($p<0.002$) indicates that NS-iCMCs are highly arrhytmic in culture. These results indicate that the functional parameters of NS-iCMCs derived from patients were compromised. Altogether, our results have demonstrated that the NS-iCMCs have a mutation in their SOS1 gene and are both structurally and functionally defective.

Discussion

In order to unravel the molecular pathologic mechanisms in rare cardiac genetic diseases, specifically NS, it is necessary to generate novel iPSC cell lines carrying the germline mutations. As NS is a uncommon genetic disorder, there are practical difficulties in obtaining patient samples and culturing them. Thus, the NS-iCMCs generated in this study will be helpful to carryout functional analysis at the cellular level. Since human iPSCs are a major source for the production of cardiomyocytes (10) (11), the iCMCs can be employed to study the genetic variants (12), pathophysiological mechanisms (13), and for the development of specific therapies (14, 15).

The cardiac characteristics associated with NS are estimated to appear in 50% to 90% of patients (16, 17). The most common cardiac abnormality in about 50–60% of NS patients is pulmonic valve stenosis. About 20% of the NS patients' exhibit hypertrophic cardiomyopathy, and about 6–10% of them show atrial septal defect (18). The other less common cardiac features associated with NS are ventricular septal defect, atrioventricular canal defect, and aortic coarctation (16, 17). SOS1 has been identified as a major gene causing NS (5), and the mutations in SOS1 had been attributed to the development of

cardiomyopathy and congenital heart defects such as valvular dysplasia, and atrial and ventricular septal defects (9).

Our study results have demonstrated that patients with NS exhibit a variant in the SOS1 gene at c.1654A>G, which could be contributing, at least partially, to the development of abnormal iCMCs. Moreover, we also observed defects in sarcomere organization and contractile function, along with a differential expression of various structural and functional genes (Fig. 5–7). These results are in accordance with other studies, where fragmented myofibrils and Z-band disruption have been documented in NS patient with cardiomyopathy and cardiac dysfunction (19). Our study results show that the expression of several important cardiac structural genes or proteins such as tropomyosin1, cardiac troponin T, α-sarcomeric actin, α-myosin heavy chain, β-myosin heavy chain, cardiac myosin-binding protein C, cardiac LIM Protein, and the regulatory molecules like GATA4, VANGL2, WWTR1 were significantly decreased in NS-iCMCs. On the other hand, cardiac hypertrophy related transcription factors like NPPA, HAND2, have been upregulated in NS patient-derived iCMCs. However, further studies warrant the effect of these individual structural and regulatory genes in exhibiting the characteristic cardiac phenotypes in NS patients.

Alteration in calcium, sodium and potassium ion channels activation genes such as HCN4, CACNA1D, CAMK2B, KCNJ5, SCN5A and CACNA1S could cause a modification in the sensitivity to these ions and lead to cardiac arrhythmias in NS-iCMCs (20–23). Although we have not performed any electrophysiological studies with our iCMCs, however, PIV method of analyzing the contractility and qRT-PCR array results may partially explain the electrocardiographic abnormalities such as wide QRS complexes and giant Q waves previously observed in 87% of NS patients (16, 24, 25). The sudden death that was observed in a patient with NS was associated with ventricular fibrillation and hypertrophic cardiomyopathy (26).

In contrast, another study has shown that SOS1 lesions do not contribute to the occurrence of congenital cardiac anomalies (27). Two other studies have shown that the NS-iCMCs with a mutation at different genes exhibited abnormal cardiac phenotypes. The mutation in RAF1 p.S257L generated iCMCs showed structural defects including myofibrillar disarray (28), and the mutation in MRAS gene at p.Gly23Val produced iCMCs characterized by an increased size and impaired calcium handling (29). Recently, Hanses et al repaired the mutations in leucine zipper-like transcription regulator 1 (LZTR1) through CRISPR in the iCMCs derived from NS patients and rescued the hypertrophic phenotype (30). In the current study, we have identified the mutation in SOS1 gene in the cells from NS patient, however, we have not unraveled the NS-patient’s cells for the presence of mutations in other genes such as RAF1 and MRAS.

It has been shown that the late-stage human iCMCs cultured for 80–120 days were shown to be more matured, compared to their early stage counterparts cultured for 20–40 days (31). Recently, we have shown that structurally and functionally developed human iCMCs can be obtained by day-30 (7). In this study, with minor modifications in our earlier protocol, we have generated structural and functional matured iCMCs on day-14 from iPSCs. We understand that the limitation of this study is devoid of an isogenic cell line with the

CRISPR-corrected mutation at the SOS1 gene variant c.1654A>G as an ideal control for comparing the phenotypic changes observed in NS patient derived cells. Although, we have employed a well characterized and established neonatal male human skin fibroblasts-derived iPSCs and iCMCs as control (7), to compare the effect of NS patient-derived cells of a female baby.

In conclusion, we have generated a human iPSC line from a patient with NS using xeno-free, non-integrating, non-viral transfection techniques. We have characterized that this iPSC line derived from the NS patient carries a specific mutation in the SOS1 gene at the c.1654A>G. This iPSC line can be used as a cell-based model for drug development to treat NS. Furthermore, we have generated and demonstrated that the NS-iCMCs were structurally and functionally defective in expressing several important cardiac structural and functional genes (Fig. 6, 7). Although further studies are required to delineate the mechanisms of functional impairment in NS-iCMCs, these NS-iCMCs can be used as a NS disease modeling platform to study the pathologic mechanisms associated with the development of cardiomyopathy and subsequently to identify novel molecular therapeutic targets. These advances will be an instrumental in helping the researchers understand rare disorders, and reassure patients and their parents by identifying a biologic basis for these diseases. Although studies are already available for NS specific iPSCs from patients with different gene variants (20–23), however, iPSCs derived CMCs from SOS1 gene mutation is novel. This in vitro cell model will also provide an opportunity to customize NS patient-specific drugs for cardiac related disease treatment. Furthermore, gene correction using clustered regularly interspaced short palindromic repeats (CRISPR) technology can be applied to correct the SOS1 gene mutation at the c.1654A>G in order to gain further insight into this rare genetic disorder. Importantly, our study results shed enough light for the future studies to uncover the molecular mechanisms associated with development and eventually to find a possible treatment for NS.

Supplementary Material

Refer to Web version on PubMed Central for supplementary material.

Acknowledgments

Funding: This work was supported in part, by American Heart Association Grant-in-Aid 16GRNT30950010 and National Institute of Health R01 grant HL141345 to JR.

References:

1. Noonan JA. (1968) Hypertelorism with Turner phenotype. A new syndrome with associated congenital heart disease. Am J Dis Child 116, 373–380 [PubMed: 4386970]
2. Mendez HM, and Opitz JM. (1985) Noonan syndrome: a review. Am J Med Genet 21, 493–506 [PubMed: 3895929]
3. El Bouchikhi I, Belhassan K, Moufid FZ, Iraqui Houssaini M, Bouguenouch L, Samri I, Atmani S, and Ouldim K. (2016) Noonan syndrome-causing genes: Molecular update and an assessment of the mutation rate. Int J Pediatr Adolesc Med 3, 133–142 [PubMed: 30805484]
4. Tartaglia M, Zampino G, and Gelb BD. (2010) Noonan syndrome: clinical aspects and molecular pathogenesis. Mol Syndromol 1, 2–26 [PubMed: 20648242]

5. Roberts AE, Araki T, Swanson KD, Montgomery KT, Schiripo TA, Joshi VA, Li L, Yassin Y, Tamburino AM, Neel BG, and Kucherlapati RS. (2007) Germline gain-of-function mutations in SOS1 cause Noonan syndrome. Nat Genet 39, 70–74 [PubMed: 17143285]

6. Yamamoto GL, Aguena M, Gos M, Hung C, Pilch J, Fahiminiya S, Abramowicz A, Cristian I, Buscarilli M, Naslavsky MS, Malaquias AC, Zatz M, Bodamer O, Majewski J, Jorge AA, Pereira AC, Kim CA, Passos-Bueno MR, and Bertola DR. (2015) Rare variants in SOS2 and LZTR1 are associated with Noonan syndrome. J Med Genet 52, 413–421 [PubMed: 25795793]

7. Rajasingh S, Thangavel J, Czirok A, Samanta S, Roby KF, Dawn B, and Rajasingh J. (2015) Generation of Functional Cardiomyocytes from Efficiently Generated Human iPSCs and a Novel Method of Measuring Contractility. PloS one 10, e0134093 [PubMed: 26237415]

8. Czirok A, Isai DG, Kosa E, Rajasingh S, Kinsey W, Neufeld Z, and Rajasingh J. (2017) Optical-flow based non-invasive analysis of cardiomyocyte contractility. Scientific reports 7, 10404 [PubMed: 28871207]

9. Baban A, Olivini N, Lepri FR, Cali F, Mucciolo M, Digilio MC, Calcagni G, di Mambro C, Dallapiccola B, Adorisio R, Novelli A, and Drago F. (2019) SOS1 mutations in Noonan syndrome: Cardiomyopathies and not only congenital heart defects! Report of six patients including two novel variants and literature review. Am J Med Genet A 179, 2083–2090 [PubMed: 31368652]

10. Mazzotta S, Lynch AT, and Hoppler S. (2018) Cardiomyocyte Differentiation from Human Embryonic Stem Cells. Methods Mol Biol 1816, 67–78 [PubMed: 29987811]

11. Hatani T, Miki K, and Yoshida Y. (2018) Induction of Human Induced Pluripotent Stem Cells to Cardiomyocytes Using Embryoid Bodies. Methods Mol Biol 1816, 79–92 [PubMed: 29987812]

12. Ma N, Zhang JZ, Itzhaki I, Zhang SL, Chen H, Haddad F, Kitani T, Wilson KD, Tian L, Shrestha R, Wu H, Lam CK, Sayed N, and Wu JC. (2018) Determining the Pathogenicity of a Genomic Variant of Uncertain Significance Using CRISPR/Cas9 and Human-Induced Pluripotent Stem Cells. Circulation 138, 2666–2681 [PubMed: 29914921]

13. Seeger T, Shrestha R, Lam CK, Chen C, McKeithan WL, Lau E, Wnorowski A, McMullen G, Greenhaw M, Lee J, Oikonomopoulos A, Lee S, Yang H, Mercola M, Wheeler M, Ashley EA, Yang F, Karakikes I, and Wu JC. (2019) A Premature Termination Codon Mutation in MYBPC3 Causes Hypertrophic Cardiomyopathy via Chronic Activation of Nonsense-Mediated Decay. Circulation 139, 799–811 [PubMed: 30586709]

14. Gramlich M, Pane LS, Zhou Q, Chen Z, Murgia M, Schotterl S, Goedel A, Metzger K, Brade T, Parrotta E, Schaller M, Gerull B, Thierfelder L, Aartsma-Rus A, Labeit S, Atherton JJ, McGaughran J, Harvey RP, Sinnecker D, Mann M, Laugwitz KL, Gawaz MP, and Moretti A. (2015) Antisense-mediated exon skipping: a therapeutic strategy for titin-based dilated cardiomyopathy. EMBO Mol Med 7, 562–576 [PubMed: 25759365]

15. Min YL, Li H, Rodriguez-Caycedo C, Mireault AA, Huang J, Shelton JM, McAnally JR, Amoasii L, Mammen PPA, Bassel-Duby R, and Olson EN. (2019) CRISPR-Cas9 corrects Duchenne muscular dystrophy exon 44 deletion mutations in mice and human cells. Sci Adv 5, eaav4324 [PubMed: 30854433]

16. Colquitt JL, and Noonan JA. (2014) Cardiac findings in Noonan syndrome on long-term follow-up. Congenit Heart Dis 9, 144–150 [PubMed: 23750712]

17. Noonan JA. (1994) Noonan syndrome. An update and review for the primary pediatrician. Clin Pediatr (Phila) 33, 548–555 [PubMed: 8001324]

18. Pierpont ME, and Digilio MC. (2018) Cardiovascular disease in Noonan syndrome. Curr Opin Pediatr 30, 601–608 [PubMed: 30024444]

19. Kawano H, Kawamura K, Ishijima M, Hayashi T, Abe K, Kawai K, and Maemura K. (2016) Myocardial fragmentation associated with disruption of the Z-band in hypertrophic cardiomyopathy in Noonan syndrome. Cardiovasc Pathol 25, 329–332 [PubMed: 27216919]

20. DiFrancesco D. (2015) HCN4, Sinus Bradycardia and Atrial Fibrillation. Arrhythm Electrophysiol Rev 4, 9–13 [PubMed: 26835093]

21. Charpentier F, Bourge A, and Merot J. (2008) Mouse models of SCN5A-related cardiac arrhythmias. Prog Biophys Mol Biol 98, 230–237 [PubMed: 19041666]

22. Hasdemir C, Aydin HH, Celik HA, Simsek E, Payzin S, Kayikcioglu M, Aydin M, Kultursay H, and Can LH. (2010) Transcriptional profiling of septal wall of the right ventricular outflow

tract in patients with idiopathic ventricular arrhythmias. Pacing Clin Electrophysiol 33, 159–167 [PubMed: 19889179]

23. Yamada N, Asano Y, Fujita M, Yamazaki S, Inanobe A, Matsuura N, Kobayashi H, Ohno S, Ebana Y, Tsukamoto O, Ishino S, Takuwa A, Kioka H, Yamashita T, Hashimoto N, Zankov DP, Shimizu A, Asakura M, Asanuma H, Kato H, Nishida Y, Miyashita Y, Shinomiya H, Naiki N, Hayashi K, Makiyama T, Ogita H, Miura K, Ueshima H, Komuro I, Yamagishi M, Horie M, Kawakami K, Furukawa T, Koizumi A, Kurachi Y, Sakata Y, Minamino T, Kitakaze M, and Takashima S. (2019) Mutant KCNJ3 and KCNJ5 Potassium Channels as Novel Molecular Targets in Bradyarrhythmias and Atrial Fibrillation. Circulation 139, 2157–2169 [PubMed: 30764634]
24. Sanchez-Cascos A. (1983) The Noonan syndrome. Eur Heart J 4, 223–229 [PubMed: 6884370]
25. Sharland M, Burch M, McKenna WM, and Paton MA. (1992) A clinical study of Noonan syndrome. Arch Dis Child 67, 178–183 [PubMed: 1543375]
26. Aydin A, Yilmazer MS, and Gurol T. (2011) Sudden death in a patient with Noonan syndrome. Cardiol Young 21, 233–234 [PubMed: 21205420]
27. Lepri F, De Luca A, Stella L, Rossi C, Baldassarre G, Pantaleoni F, Cordeddu V, Williams BJ, Dentici ML, Caputo V, Venanzi S, Bonaguro M, Kavamura I, Faienza MF, Pilotta A, Stanzial F, Faravelli F, Gabrielli O, Marino B, Neri G, Silengo MC, Ferrero GB, Torrrente I, Selicorni A, Mazzanti L, Digilio MC, Zampino G, Dallapiccola B, Gelb BD, and Tartaglia M. (2011) SOS1 mutations in Noonan syndrome: molecular spectrum, structural insights on pathogenic effects, and genotype-phenotype correlations. Hum Mutat 32, 760–772 [PubMed: 21387466]
28. Jaffre F, Miller CL, Schanzer A, Evans T, Roberts AE, Hahn A, and Kontaridis MI. (2019) Inducible Pluripotent Stem Cell-Derived Cardiomyocytes Reveal Aberrant Extracellular Regulated Kinase 5 and Mitogen-Activated Protein Kinase Kinase 1/2 Signaling Concomitantly Promote Hypertrophic Cardiomyopathy in RAF1-Associated Noonan Syndrome. Circulation 140, 207–224 [PubMed: 31163979]
29. Higgins EM, Bos JM, Dotzler SM, John Kim CS, and Ackerman MJ. (2019) MRAS Variants Cause Cardiomyocyte Hypertrophy in Patient-Specific Induced Pluripotent Stem Cell-Derived Cardiomyocytes: Additional Evidence for MRAS as a Definitive Noonan Syndrome-Susceptibility Gene. Circ Genom Precis Med 12, e002648 [PubMed: 31638832]
30. Hanses U, Kleinsorge M, Roos L, Yigit G, Li Y, Barbarics B, El-Battrawy I, Lan H, Tiburcy M, Hindmarsh R, Lenz C, Salinas G, Diecke S, Muller C, Adham I, Altmuller J, Nurnberg P, Paul T, Zimmermann WH, Hasenfuss G, Wollnik B, and Cyganek L. (2020) Intronic CRISPR Repair in a Preclinical Model of Noonan Syndrome-Associated Cardiomyopathy. Circulation 142, 1059–1076 [PubMed: 32623905]
31. Lundy SD, Zhu WZ, Regnier M, and Laflamme MA. (2013) Structural and functional maturation of cardiomyocytes derived from human pluripotent stem cells. Stem cells and development 22, 1991–2002 [PubMed: 23461462]

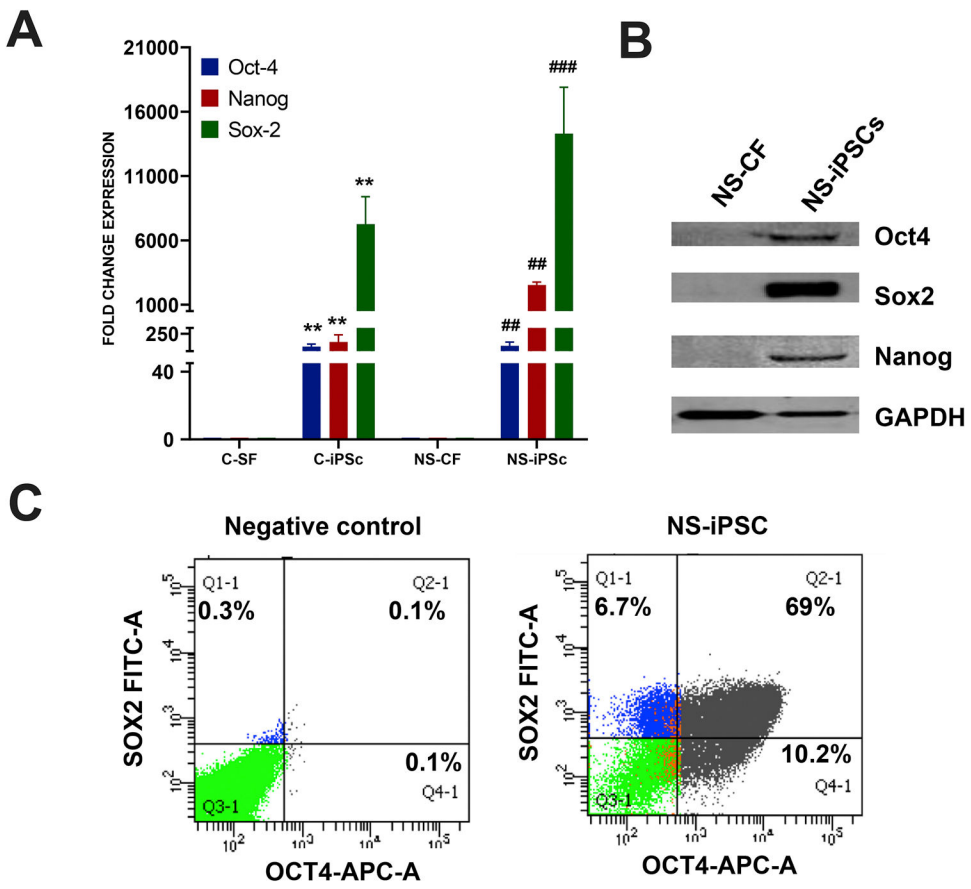

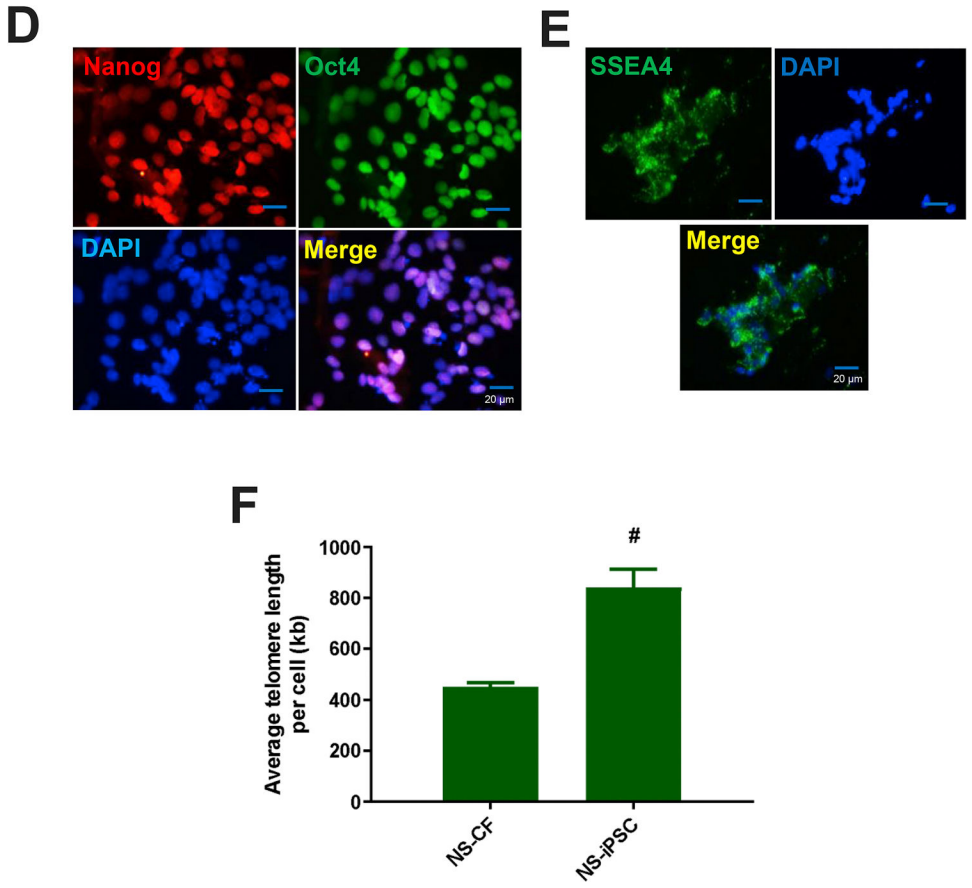

Figure 1. Characterization of the pluripotency of iPSCs derived from NS patient.

(A) The qRT-PCR analyses show the mRNA fold expression of pluripotency genes OCT4, Nanog and Sox2 were significantly increased in iPSCs derived from normal control human skin fibroblasts (C-SF) and Noonan syndrome patients' cardiac fibroblasts (NS-CF) when compared to their respective parent cells. Fold mRNA expression was calculated as the ratio of NS-iPSCs expression to parent NS-CF. 18S rRNA was used as endogenous control. Each bar represents mean ± SEM of three replicated experiments. **P<0.01, ***P<0.001 vs. C-SF; $^{\#\#}$P<0.01, $^{\#\#\#}$P<0.001 vs. NS-CF. (B) Western blot analysis showed that the endogenous pluripotent genes Nanog, Sox2 and OCT4 were activated in NS-iPSCs when compared with its non-reprogrammed parent cells (NS-CF). GAPDH was used as endogenous control. (C) Flow cytometric analysis demonstrated that around 86% cells were expressing either double positive Oct4 and Sox2 or Oct4 alone or Sox2 alone in NS-iPSCs. The cells stained with secondary antibody alone were used as negative control. (D-E) Similarly, the immunofluorescence analyses showed that NS-iPSCs were positively stained for pluripotency markers Nanog and Oct4 (D), and SSEA4 (E), and the DAPI staining was performed to visualize the nucleus. Scale bar: 20 µm (F) Absolute telomere length measurement was measured with specific primers sets using qRT-PCR. The telomere length was significantly increased in NS-iPSCs when compared to NS-CF. $^{\#}$P<0.05 vs. NS-CF.

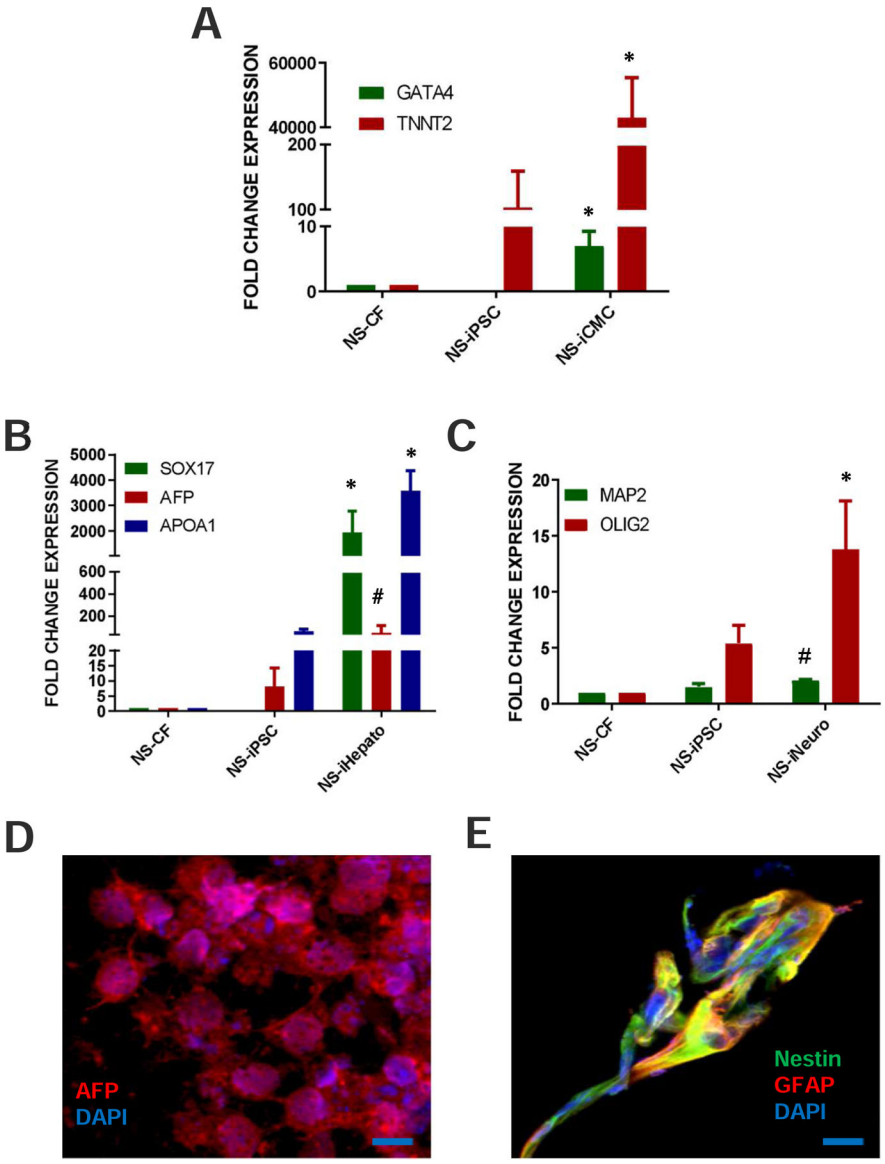

Figure 2. Tri-lineage differentiation capabilities of NS-iPSCs.

(A-C) NS-iPSCs were cultured in either cardiac-specific (mesoderm), or hepatocyte-specific or neuronal-specific (ectoderm) differentiation medium for 21 days, followed by qRT-PCR analyses. Our qRT-PCR data demonstrated that the induction of cardiac gene GATA4 and TNNT2 (A), hepatocyte gene SOX17, AFP, and APOA1 (B), and neuronal specific genes MAP2 and (C) were significantly expressed in iPSCs cultured under their respective differentiation medium when compared to their control NS-CF and NS-iPSCs. 18S rRNA was used as endogenous control. Each bar represents mean ± SEM of three replicated experiments. *P<0.05 vs. their respective NS-CF and NS-iPSC; #P<0.05 vs. their respective NS-CF. (D-E) Immunofluorescence analysis demonstrated the differentiation capabilities of NS-iPSCs into hepatocytes (D), and neuronal (E) specific cells, under the specific differentiation conditions. Scale bar: 20 μm

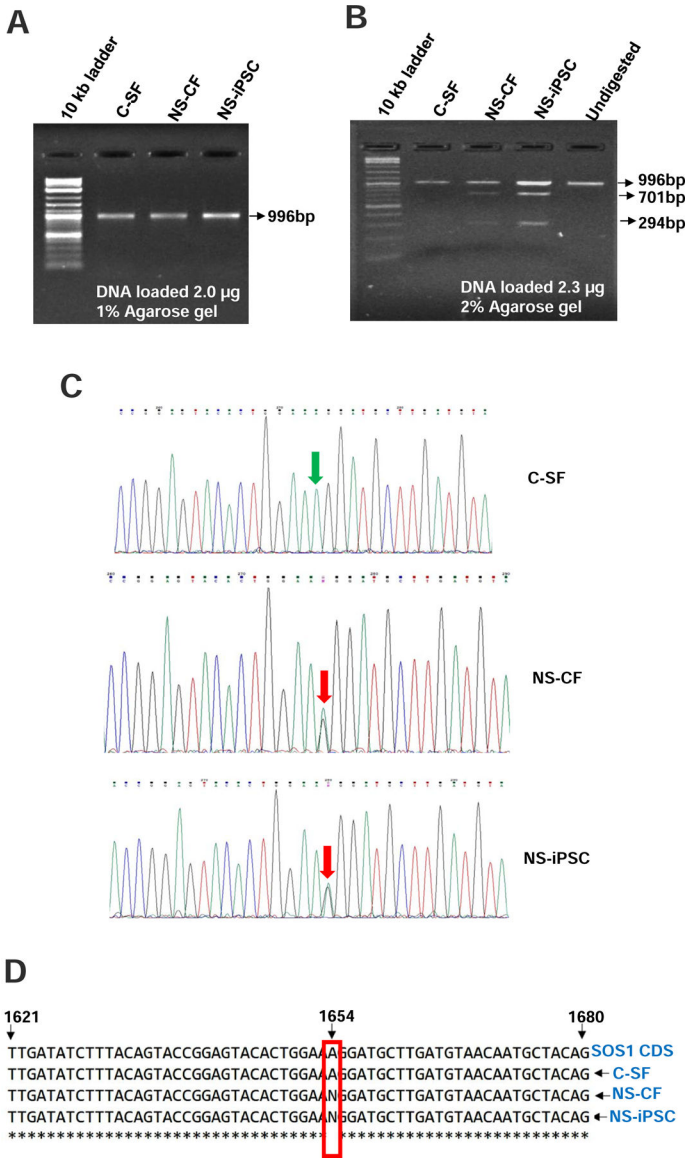

Figure 3. Identification of the SOS1 gene mutation in NS patients.

(A) SOS1 gene-specific primes were designed and used to amplify the 996bp containing the SOS1 gene variant (rs137852814). Lane-1, 10kb ladder, Lane-2, control skin fibroblasts C-SF), Lane-3, NS cardiac fibroblasts (NS-CF) and Lane-4, NS-iPSCs (NS-iPSC). (B) The PCR product obtained in Fig.3A was digested with the restriction enzyme *HpyAV*, and analyzed by restriction fragment length polymorphism. Lane-1, 10kb ladder, Lane-2, control skin fibroblasts (C-SF), Lane-3, NS cardiac fibroblasts (NS-CF), Lane-4, NS-iPSCs (NS-iPSC), and Lane-5, undigested sample. (C) Sanger sequencing chromatogram of the SOS1 gene PCR product from Fig. 3A showed that homozygous wild-type (A/A) was present in control skin fibroblasts (C-SF) (indicated by green arrow), and a heterozygous mutant-type (A/G) was present in NS cardiac fibroblasts (NS-CF) and NS-iPSCs (indicated by red arrows). (D) The sequence of PCR products from Fig. 3A were aligned with SOS1 coding sequence using multiple sequence alignment tool Clustal Omega, which indicated

that C-SF sequence was matched with SOS1 wildtype sequence, whereas a gap at 1654 (highlighted with a red rectangle) was seen in NS-CF and NS-iPSCs sequences.

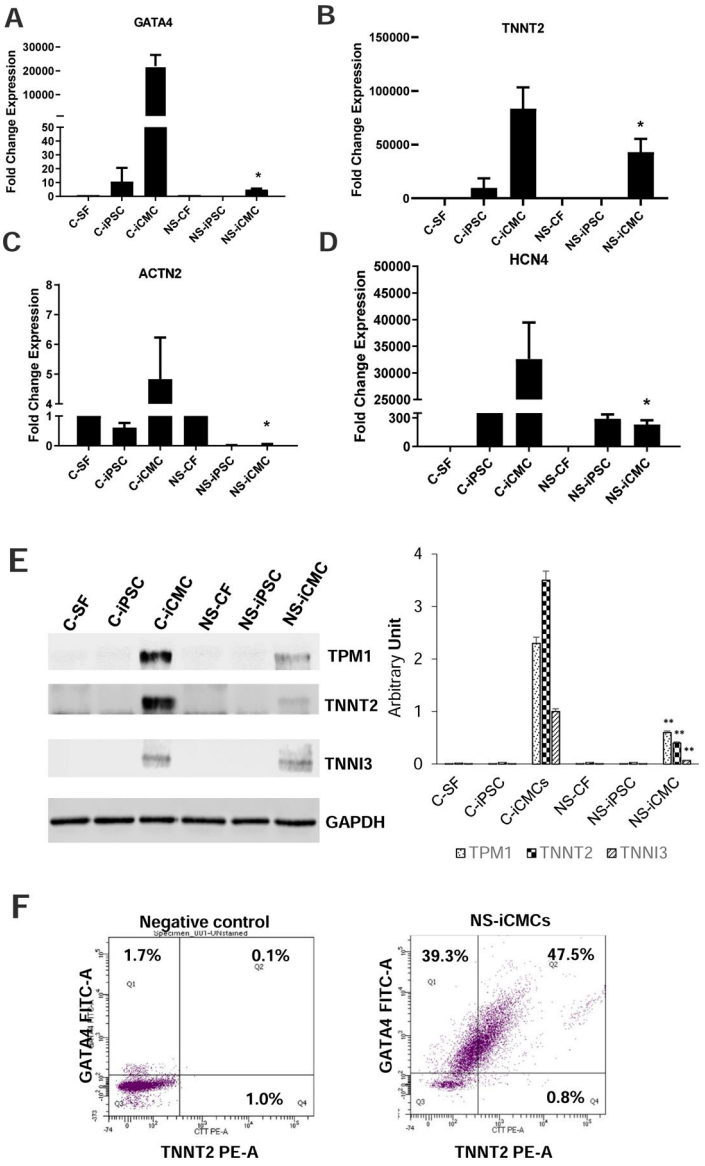

Figure 4. The Cardiac specific genes are significantly lower in NS-iCMCs.

(A-D) Quantitative qRT-PCR data showed that the expression of cardiac genes Gata4 (A), cardiac troponin T (TNNT2) (B), hyperpolarization activated cyclic nucleotide gated potassium channel 4 (HCN4) (C) and α-sarcomeric actinin (ACTN2) (D) in Noonan Syndrome (NS) patient-derived induced cardiomyocytes (NS-iCMCs) were significantly reduced when compared to the control (C-iCMCs). 18S rRNA was used as endogenous control. Each bar represents mean ± SEM of three replicated experiments. *P<0.05 vs. their respective C-iCMC. (E) Western blotting and graphical analyses showed that the expression of cardiac proteins tropomyosin1 (TPM1), cardiac troponin T (TNNT2) and cardiac troponin I (TNNI3) were significantly reduced in NS-iCMCs when compared to the control C-iCMCs. GAPDH was used as endogenous control. Each bar represents mean ± SEM of three replicated experiments. **P<0.01 NS-iCMCs vs. their respective C-iCMCs. (F) FACS analyses revealed the proportion of cells expressing cardiac proteins such as

GATA4 and cardiac troponin T (TNNT2) in NS-iCMCs. The cells stained with secondary antibody alone were used as negative control.

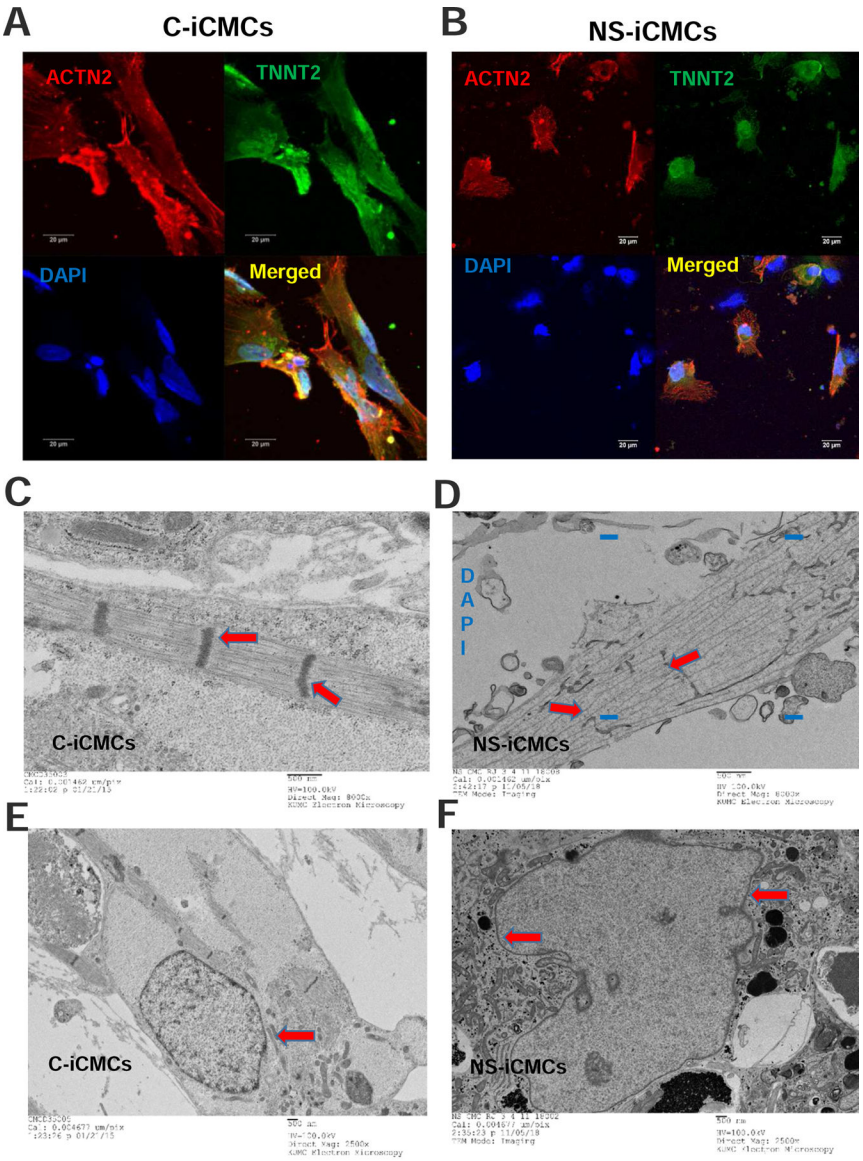

Figure 5. The ultrastructural image analysis of day 14 C-iCMCs and NS-iCMCs demonstrates that the NS-iMCS were structurally disorganized.

(A-B) Immunofluorescence analysis for the expression of alpha sarcomeric actinin (ACTN2-red), TNNT2 (green) and nuclear staining (DAPI-blue) in C-iCMCs and NS iCMCs on day 14. Scale bar: 20 μm (C-D) The electron microscopic images depicting that the C-iCMCs show a high density of sarcomeres well aligned along the myofibrils (C) whereas, in NS-iCMCs, the sarcomeres were disorganized and irregularly spaced (D) asindicated by red arrows. (E-F) The electron microscopic images also showing the differences in the structure of nucleus (indicated by red arrows) in control and NS-patient derived iCMCs. The representative images are from three repeated experiments.

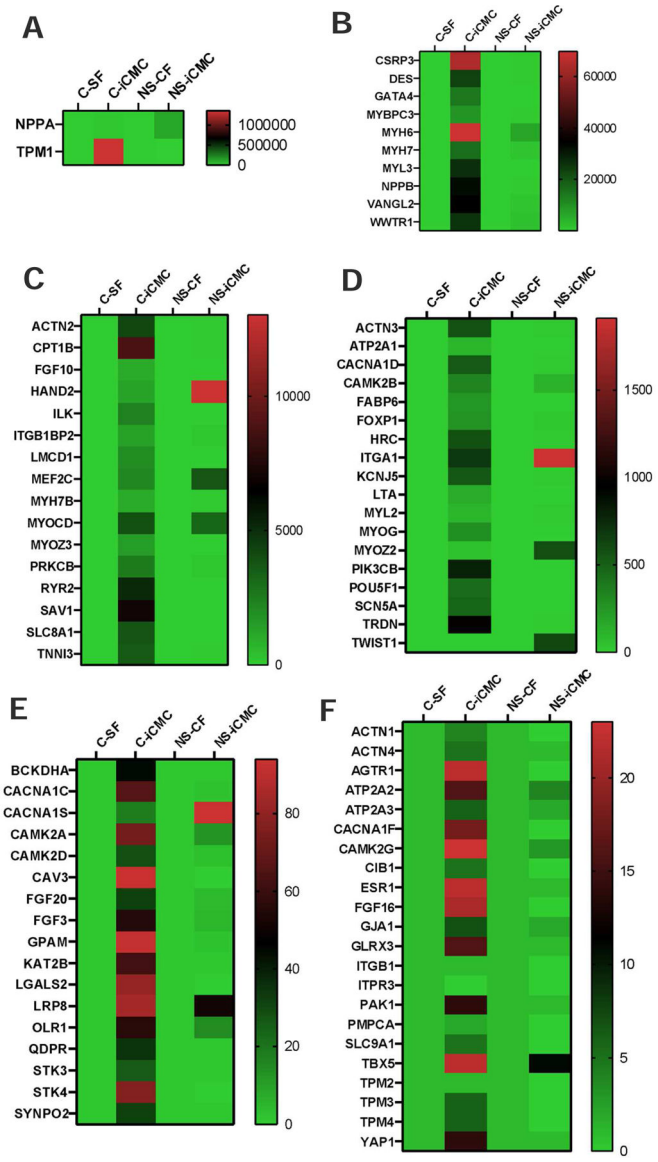

Figure 6. The expression of Cardiac specific gene transcripts were significantly reduced in NS-iCMCs.

(A-F) Comparative Heatmap analyses depicting the mRNA expression profile of various cardiac myocyte genes in induced cardiomyocytes (iCMCs)-derived from control (C) and Noonan Syndrome (NS) patient. Three samples from each group were analyzed through qPCR array, and the mean mRNA fold expression levels are depicted in the heatmap. Each gene expression was normalized with GAPDH, and the fold change in gene expression in iCMCs were normalized with their respective parent cell types. The qPCR array results have been classified based on the level of expression genes.

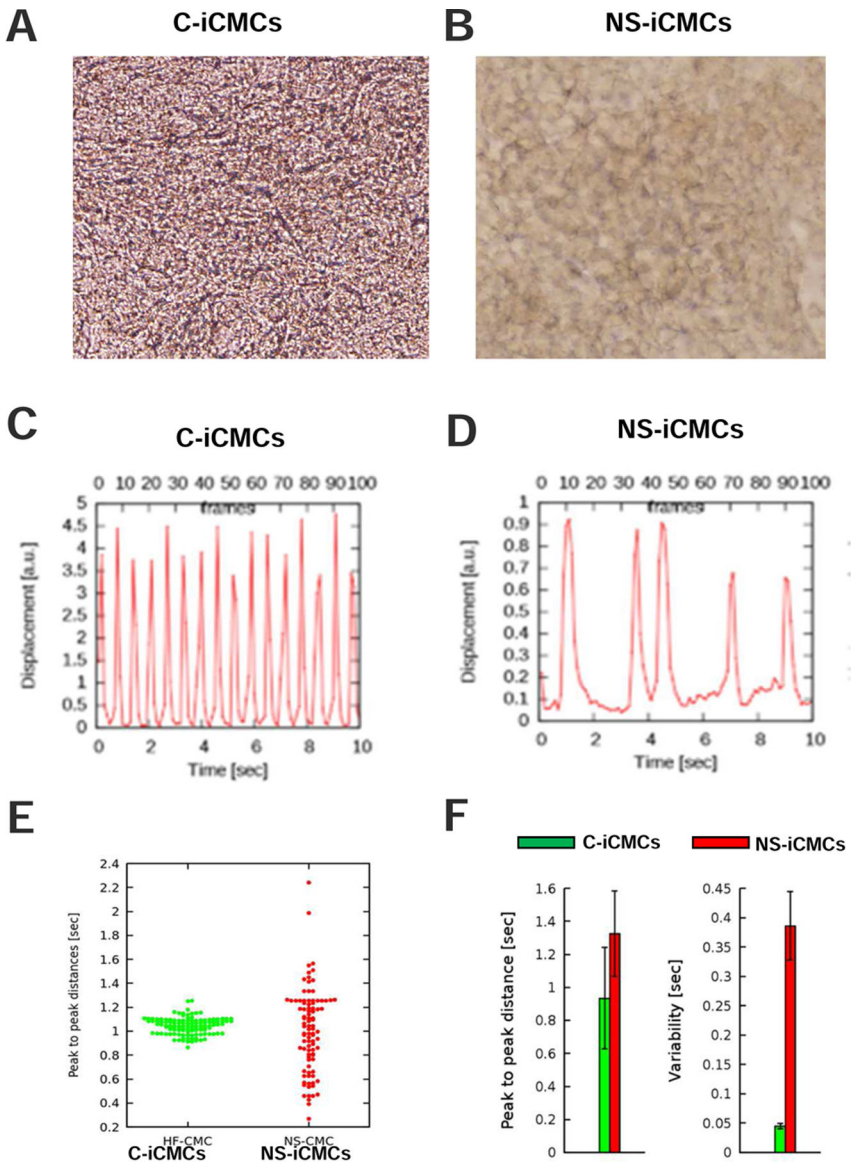

Figure 7. The contractility of NS-iCMCs were functionally defective.

(A-D) We utilized a non-invasive optical assay based on particle image velocimetry (PIV) analysis of video microscopic recordings for the purpose of quantifying the contraction of iCMCs-derived from control (C) and Noonan Syndrome (NS) patient-derived iCMCs. Representative video microscopic fields (A and B) and their characteristic beat patterns; Scale bar: 50 μm (C and D) are shown for C-iCMCs (A and C) and of NS-iCMCs, (B and D). While the beat intervals (peak-to-peak distances) of C-iCMCs are regular, NS-iCMCs exhibit profound arrhythmia. The duration of each individual beat intervals are pooled from n=6 independent recordings and plotted in a bee swarm plot (E), which indicate a much broader distribution of beat intervals in NS-iCMC cultures. The mean and standard deviation of the beat intervals are compared on a histogram (F), indicating that the beat intervals of NS-iCMCs are slightly longer ($p=0.3$), their standard deviation is 7-fold increased when compared to C-iCMCs ($p<0.002$).

Table 1

Primers used for qPCR using SYBR Green.

Category	Gene Symbol	Gene primers used for SYBR Green qPCR Assay	
		Forward (5′ to 3′)	Reverse (5′ to 3′)
House keeping	18S	CTACCACATCCAAGGAAGCA	TTTTTCGTCACTACCTCCCCG
Pluripotency	OCT4	TGTTCCCAATTCCTTCCTTAGTG	TGCCAGGGTTTTTGGGATTAAGTT
	NANOG	AAAGGCAAACAACCCACT	GCTATTCTTCGGCCAGTT
	SOX2	CAGCGCATGGACAGTTAC	GGAGTGGGAGGAAGAGGT
Cardiomyocyte	TNNT2	GGCAGCGGAAGAGGATGCTGAA	GAGGCACCAAGTTGGGCATGAACGA
	GATA4	TACATCAGCTTCCGGAACCACCAA	GGAGGAACTGTCGCGAAGATCAAA
	ACTN2	GAGCAGATCTTGCTGCAGAAG	CCAGGAAACAAACTGTGACTTC
	HCN4	AGAGCGCGTAGGAGTACTGCTT	GACTGCTGGGTGTCCATCAA
Endoderm markers	SOX17	CTCTGCCTCCTCCACGAA	CAGAATCCAGACCTGCACAA

Table 2

Primers used for Taqman qPCR assay.

Category	Gene Symbol	Gene primers used for TaqMan qPCR Assay
House keeping	18S	Hs03928985_g1
Endoderm markers	AFP	Hs01040607_m1
	APOA1	Hs00985000_g1
Neuronal markers	MAP2	Hs00258900_m1
	OLIG2	Hs00300164_s1